Direct measurement of anisotropic near-wall hindered diffusion using total internal reflection velocimetry

Peter Huang* and Kenneth S. Breuer
Division of Engineering, Brown University, Providence, Rhode Island 02912, USA
(Received 10 February 2007; published 6 October 2007)

By applying the three-dimensional total internal reflection velocimetry (3D-TIRV) technique to freely suspended micron-sized fluorescent particles, we are able to simultaneously observe the three-dimensional anisotropic hindered diffusion for values of the gap-size-to-radius ratio much less than one. We demonstrate that the 3D-TIRV can be used to accurately track freely suspended 1.5-μm radius particles. The displacement measurements reveal that the hindered diffusion coefficients are in close agreement with the theoretical values predicted by the asymptotic solutions of Brenner [Chem. Eng. Sci. **16**, 242 (1961)] and Goldman *et al.* [Chem. Eng. Sci. **22**, 637 (1967)] for gap-size-to-radius ratio much less than one, while hindered diffusion anisotropicity is simultaneously observed in all data sets.

DOI: 10.1103/PhysRevE.76.046307 PACS number(s): 47.57.−s, 47.61.−k, 66.10.−x

I. INTRODUCTION

Advancements in colloidal sciences have led to many applications in which micron and nanometer sized particles are used in close proximity to solid surfaces. At these length scales, Brownian motions are significant and understanding these thermal agitations are essential in making practical use of these tiny particles. This is particularly true for particle tracking applications, such as particle tracking velocimetry (PTV) when Brownian motion can induce important bias [1,2]. In the fluid bulk, the diffusivity of an isolated particle follows the Stokes-Einstein relation, which balances the fluid thermal energy with the particle's hydrodynamic mobility. In the presence of a nearby solid boundary, however, a particle experiences an increased, anisotropic drag which hinders its mobility. Brenner [3] and Goldman *et al.* [4] were the first to develop drag force correction factors for near-wall spheres under no inertial effects and a no-slip boundary condition. These correction factors have since evolved into theories of hindered diffusion [5].

Following these works, many experimental studies have been conducted to observe hindered diffusion and to verify the correction factors. Demonstrated experimental techniques include evanescent light scattering [6–8], total internal reflection fluorescence microscopy (TIRFM) [9,10], and combined optical tweezers and digital video microscopy [11]. In most of the above-mentioned studies, simultaneous three-dimensional measurements of the anisotropic diffusivity could not be conducted due to experimental limitations. One exception is a ratiometric-TIRFM measurement conducted by Banerjee and Kihm [9], who reported anisotropic diffusivities that only partially agree with the theories, probably due to limitations in their measurement techniques. Another exception is a study reported by Lin *et al.* [11], who demonstrated that the effects of anisotropic hindered diffusion extend far from the wall.

In the theories of Brenner and Goldman *et al.* the hindered mobility of a near-wall particle is a function of the particle's radius, a, and the gap size between the particle and the wall, h. They proposed analytical solutions of the hindered mobility that are vastly different for $h/a \gtrsim 1$ and for $h/a \ll 1$. To our knowledge, no experimental study has measured the three-dimensional anisotropic hindered diffusion for $h/a \ll 1$. In this paper we present such measurements, aimed to validate the anisotropic mobility correction coefficients for $h/a \ll 1$ through a direct measurement of hindered diffusion using three-dimensional total internal reflection velocimetry (3D-TIRV).

II. THEORY OF HINDERED DIFFUSION

When an isolated particle is at the vicinity of a solid boundary, its Brownian motion is hindered due to an increase in hydrodynamic drag. The presence of the solid wall also breaks the symmetry of particle dynamics, resulting in anisotropic Brownian motion. Brenner [3] successfully solved the lubrication equation of particle motion normal to the solid wall and proposed an infinite series solution of the drag correction factor, $\beta_\perp$. He reported that the correction factor is a function of the particle radius, a, and the gap size between the particle and the solid wall, h. Later Bevan and Prieve [6], using a regression method, reported that

$$\beta_\perp \equiv \frac{D_\perp}{D_0} \approx \frac{6\left(\frac{h}{a}\right)^2 + 2\left(\frac{h}{a}\right)}{6\left(\frac{h}{a}\right)^2 + 9\left(\frac{h}{a}\right) + 2} \tag{1}$$

is a close approximation to Brenner's infinite series solution. For the diffusivity correction factor in the direction parallel to the solid wall, $\beta_\parallel$, an exact analytical solution was never found. Instead, Goldman *et al.* [4] offered an asymptotic solution,

$$\beta_\parallel \equiv \frac{D_\parallel}{D_0} = -\frac{2\left[\ln\left(\frac{h}{a}\right) - 0.9543\right]}{\left[\ln\left(\frac{h}{a}\right)\right]^2 - 4.325\ln\left(\frac{h}{a}\right) + 1.591}, \tag{2}$$

for particles very close to the wall, defined by $h/a \ll 1$.

*Present address: Department of Biomedical Engineering, Tufts University; peter.huang@tufts.edu

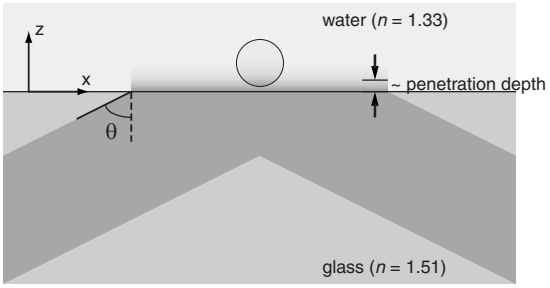

FIG. 1. Schematic of TIRV. A fluorescent microparticle suspended in water is placed in an evanescent field created within the focal depth of a high numerical aperture microscopy objective. A collimated laser beam through the objective is used as the illumination light source. At the illumination beam incident angle, θ, greater than 61.9°, total internal reflection occurs at the glass-water interface. Because the particle radius is much larger than the evanescent penetration depth, the evanescent energy illuminates only the lower portion of the encapsulated fluorophores.

III. EXPERIMENTAL PROCEDURES

To experimentally validate the equations for hindered diffusion [(1) and (2)], the motion of micron-sized fluorescent particles near the wall was measured using total internal reflection velocimetry (TIRV) [1]. The particles are illuminated by the evanescent field of an incident laser beam which ensures that only the near-wall region is visible (Fig. 1). Furthermore, we use the exponentially decaying illumination intensity to infer the instantaneous separation distance between the particle and the two-media interface, as commonly done in traditional TIRFM experiments [10,12]. By using relatively large particles (1.5 μm), the particles are visible only for very small values of the gap-to-radius ratio, h/a. In addition, the diffusion time scales are very slow so that particle displacements can be tracked easily using low-frequency image acquisitions.

Our 3D-TIRV setup was created using an inverted epifluorescent microscope (Nikon TE-2000). A continuous-wave, collimated 514-nm argon-ion laser beam was directed through a Nikon PL Apo NA 1.45 100× TIRF oil immersion objective at an angle that created total internal reflection at a glass-water interface. The water phase was an aqueous solution consisting of 10 mM NaCl and individual 1.5-μm-radius (±5%) fluorescent polystyrene particles (refractive index 1.59, Spherotec Inc.) suspended at 0.02% volume fraction. The low volume fraction, and thus low particle number density, ensured the isolated-particle assumption of the theories was met. Before each measurement the solution was sonicated in intervals of 30 s for 10 min to disperse coagulated particles. For image acquisition, 200 μL of the solution was injected into a closed reservoir formed by a piece of carved polydimethylsiloxane (PDMS) sandwiched between glass coverslips. Subsequently TIRV imaging of hindered particle Brownian motions was performed at one of the glass-solution interfaces. The images of the particles were captured using an intensified charge coupled device camera (Q-Imaging) and recorded at 10 Hz. Overall, 2000–2500 sample images were captured for each experiment for reliable statistics.

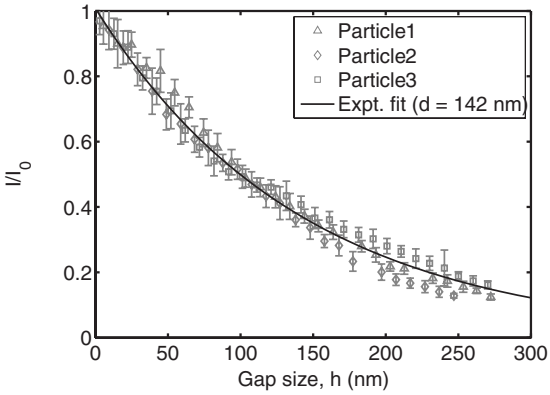

FIG. 2. Gaussian-fitted peak intensities, I, of 1.5-μm radius fluorescent particles in evanescent field, taken at 0–275 nm away from the glass surface. I_0 is the fitted intensity at $h = 0$. Each data point represents the particle peak intensity averaged over ten images, while the length of the error bar spans two standard deviations. The laser incident angle is 64° and the resulting evanescent field penetration depth is 148 nm. All data series exhibit an exponential decay tendency versus gap size. With an exponential decay length of 142 nm, the best fit of the intensity data shows close agreement to the penetration depth.

A particle's three-dimensional position was determined through threshold-identification and Gaussian fitting of the intensities of the pixels surrounding the peak. This method has been previously demonstrated in TIRV with nanoparticles [1]. Nevertheless, a calibration experiment was necessary to verify its validity for 1.5-μm particles, especially in determining the relationship between the particle-wall gap size and the particle's peak fluorescent intensity. To accomplish this, individual 1.5-μm radius fluorescent polystyrene particles were attached to polished conical tips of thin graphite rods (tip diameter approximately 100 μm). By mounting the assembly to a precision translation stage (Mad City Labs), the fluorescent particles were traversed through the evanescent field and their fluorescent images were digitally captured at various distances to the glass surface. The result of this calibration is shown in Fig. 2. The close agreement between particle intensity's exponential decay length and the evanescent field penetration depth confirms that the particle-glass gap size can be reliably inferred from the peak intensity. Using the calibration, we estimate that the precision of gap size identification was approximately 30 nm.

During the diffusion experiment, particles were tracked over several frames and once positions of all imaged particles were determined, particle displacements were calculated between consecutive frames, with an uncertainty of approximately 50 nm. The hindered diffusion coefficient in the direction parallel to the glass surface, $D_{\parallel}$, was calculated from the equation

$$\langle \Delta R \rangle^2 = \pi D_{\parallel} \Delta t, \tag{3}$$

where ΔR is radial displacement of a particle, Δt is the time between consecutive image acquisitions (=100 ms), and $\langle\ \rangle$ represents ensemble average. Similarly, the hindered diffu-

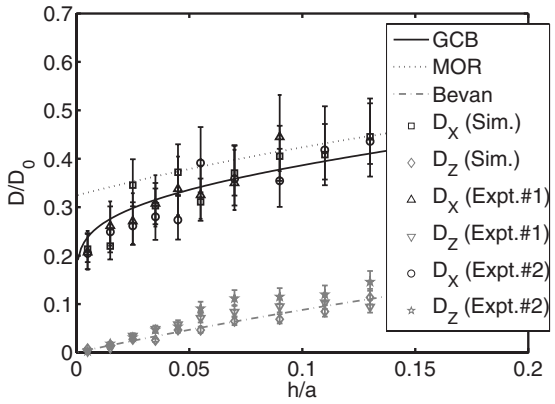

FIG. 3. Hindered diffusion correction factor (D_x/D_0, D_z/D_0) vs nondimensional gap size between particles and glass surface (h/a). D_0 is the diffusion coefficient measured in the fluid bulk while $D_x = D_\parallel$ and $D_z = D_\perp$. Each data point is obtained from an ensemble of particles found within ±0.005 or ±0.01 of the targeted gap size values. "GCB," "MOR," and "Bevan" represent the asymptotic solution of Goldman *et al.*, the Bevan approximation, and "method of reflection" solution, respectively. "Expt." represents experimental data while "Sim." means data obtained from Brownian dynamics simulation. Each error bar represents the 95% confidence interval of measurement.

sion coefficient in the direction normal to glass surface, $D_\perp$, was calculated from

$$\langle (\Delta z)^2 \rangle - \langle \Delta z \rangle^2 = 2D_\perp \Delta t, \tag{4}$$

where Δz is the particle displacement normal to the glass surface. Finally, to obtain the hindered diffusion correction factors, $\beta_\parallel$ and $\beta_\perp$, we divide by the bulk diffusion coefficient, D_0, obtained using the same techniques, with the same particles suspended in the same fluid, this time, however, imaged far from the wall using standard flood illumination.

IV. RESULTS AND DISCUSSION

Shown in Fig. 3 are hindered diffusion correction factors measured by 3D-TIRV. In addition to experimental results, hindered diffusion coefficients from a Brownian dynamics simulation [2] are also plotted for comparison. These results are compared to the asymptotic solution of Goldman *et al.* [Eq. (2)], Bevan's approximation [Eq. (1)], and a "method of reflection" (MOR) solution [4]. Theoretically Eq. (2) is more appropriate for the measured gap sizes of $h/a \ll 1$ while the method of reflection solution is more accurate at $h/a > 1$, but nevertheless they are both plotted for a quantitative comparison. The correction factor in the direction parallel to the glass surface, $\beta_\parallel \equiv D_x/D_0$, increases from approximately 0.2 at $h/a \approx 0$ to 0.4 at $h/a \approx 0.13$, while the correction factor in the direction normal to the glass surface, $\beta_\perp = D_z/D_0$, increases from 0 to 0.1 in the same h/a range, demonstrating the anisotropicity of near-wall hindered diffusion. It is observed that the measured $\beta_\parallel$ values at $h/a < 0.05$ are very close to that predicted by Eq. (2) but significantly deviate from the MOR solution, confirming the validity of the asymptotic solution at $h/a \ll 1$. The transition from the asymptotic solution to the method of reflection solution is demonstrated at $h/a > 0.1$ as the measured $\beta_\parallel$ values fall between the two solutions. The measured $\beta_\perp$ agrees well with Bevan's approximation, except at $0.05 < h/a < 0.1$ where measured $\beta_\perp$ is slightly larger than the predicted values possibly due to insufficient or slightly biased particle sampling. A close agreement between the measured and the predicted $\beta_\perp$ values at extremely small h/a has also been reported by Oetama and Walz [8], who conducted one-dimensional hindered diffusion measurement in the range $h/a < 0.025$. Finally, the experimental data also agree well with the simulation results, confirming the validity of our measurement technique.

As in most near-wall colloidal measurements, we realize the importance of recognizing other acting physical forces that could lead to measurement inaccuracy. One of these forces is gravitational pull or sedimentation of the particles. At first glance, it is perceivable that sedimentation could lead to bias in diffusion measurement normal to the glass boundary. In the fluid bulk of density ρ_f and dynamic viscosity μ, the terminal settling velocity, w_s, of a particle with radius a and density ρ_p is

$$w_s = \frac{2(\rho_p - \rho_f)ga^2}{9\mu}, \tag{5}$$

where g is the gravitational acceleration. For a 1.5-μm radius polystyrene particle of density 1050 kg/m^3, this terminal settling velocity would be 245 nm/s, equivalent to a settling displacement of 24.5 nm during the imaging interframe time of 0.1 s. However, when the particle approaches the solid boundary, its terminal velocity is expected to decrease with a correction factor identical to $\beta_\perp$ for the same hydrodynamic reason of decreased mobility. Based on Eq. (1), within the evanescent penetration depth the particles would settle for a distance of less than 2.45 nm in the interframe time of 0.1 s, or equivalently a nondimensional gap size of 0.0016 for our measurement gap size of $h/a < 0.14$. Therefore in the time scale of our Brownian motion measurements, sedimentation can be considered as a negligible factor.

Besides hydrodynamic interaction, electrostatic repulsion can also exist between the polystyrene particles and the glass surface as they both carry negative surface charges when immersed in aqueous solution [13]. Indeed when the same fluorescent particles were suspended in deionized water and observed under evanescent wave imaging, we found few particles came close to the glass surface. However, the length scale of electrostatic repulsion can be easily decreased by increasing the electrolyte concentration of the suspending aqueous solution. By adding 10 mM of NaCl to the solution, we decreased the electric double layer thickness surrounding the particles and the glass surface to a Debye length ~3 nm, or $h/a \sim 0.002$, and thus significantly reduced the effects of electrostatic repulsion.

Another colloidal force that could potentially affect measurement accuracy is van der Waals force between the particles and the glass. For a particle-glass gap size of 10 nm, van der Waals force between a flat glass and a 1.5-μm particle is approximately 10^{-10} N, or ten times smaller than the electrostatic repulsion [14]. Furthermore, at gap sizes larger

than 10 nm, van der Waals force tapers off with an h^{-3} dependency due to retardation effect, making its effective range much shorter than that of electrostatic repulsion [14,15]. Thus it is safe to assume that van der Waals force is also insignificant for the range of h/a under consideration.

The hydrodynamic mobility correction factors proposed by Brenner and Goldman *et al.* assume a no-slip boundary condition at particle surfaces. If fluid slip exists at the particle surfaces, it is expected that the theories of Brenner and Goldman *et al.* would underestimate near-surface particle mobility and the hindered diffusion coefficients. Several recent theoretical and experimental studies, however, offer insights into whether slip effect should be taken into consideration. First, by conducting slip measurements of water flowing over hydrophobic surfaces, Zhu and Granick [16] concluded that apparent slip lengths are only a few nanometers if the rms surface roughness is 3.5 nm or larger. Because the polystyrene microspheres used in the current hindered diffusion experiment are hydrophilic and have surface roughness of at least 10 nm [17], the effective slip length at particle surfaces, δ, is expected to be of only a few nanometers in magnitude, if not subnanometer. Thus under the current experimental conditions, $h/\delta \gg 10$. Consequently, based on the theory of particle mobility presented by Vinogradova [18], a slip of such magnitude would have an insignificant effect on the particle mobility for the particle diameter and particle-wall gap size under consideration. Therefore the no-slip assumption is considered valid in the current experiment, and is additionally verified by the agreement between experimental data and theoretical values shown in Fig. 3.

Finally the combination of 1.5-μm particle radius and 225-nm measurement depth in total internal reflection velocimetry was chosen to provide the optimal range of h/a in which Brownian motion is hindered but still strong enough to confirm the validity of the asymptotic solution at $h/a \ll 1$. It is expected that correction factors similar to that of Fig. 3 would be obtained if additional measurements were conducted using particle radii between 1 and 10 μm because total internal reflection velocimetry provides the same measurement accuracy within this range of particle sizes. Furthermore, magnitudes of the aforementioned particle sedimentation, electrostatic repulsion, van der Waals force, and particle surface slip are not expected to vary significantly enough to affect the correction factor measurement accuracy if an alternative particle size had been chosen. Therefore we believe the hydrodynamic mobility correction factors presented in Fig. 3 are independent of the size of the particles that experiments are conducted in.

V. SUMMARY

A direct measurement of hindered diffusion was conducted with total internal reflection velocimetry. The anisotropic characteristic of hindered diffusion is experimentally confirmed and the correction factors are found to agree with the theories of Brenner and Goldman *et al.* The results confirm the increase of hydrodynamic drag when a particle approaches a solid boundary, and such correction shall be applied to not only diffusion but also other translational motion of particles where the drag force is of concern.

[1] Peter Huang, Jeffrey S. Guasto, and Kenneth S. Breuer, J. Fluid Mech. **566**, 447 (2006).
[2] Peter Huang and Kenneth S. Breuer (to be published).
[3] Howard Brenner, Chem. Eng. Sci. **16**, 242 (1961).
[4] A. J. Goldman, R. G. Cox, and H. Brenner, Chem. Eng. Sci. **22**, 637 (1967).
[5] Nasser A. Frej and Dennis C. Prieve, J. Chem. Phys. **98**, 7552 (1993).
[6] Michael A. Bevan and Dennis C. Prieve, J. Chem. Phys. **113**, 1228 (2000).
[7] M. Hosoda, K. Sakai, and K. Takagi, Phys. Rev. E **58**, 6275 (1998).
[8] Ratna J. Oetama and John Y. Walz, J. Chem. Phys. **124**, 164713 (2006).
[9] Arindam Banerjee and Kenneth D. Kihm, Phys. Rev. E **72**, 042101 (2005).
[10] K. D. Kihm, A. Banerjee, C. K. Choi, and T. Takagi, Exp. Fluids **37**, 811 (2004).
[11] Binhua Lin, Jonathan Yu, and Stuart A. Rice, Phys. Rev. E **62**, 3909 (2000).
[12] Atom Sarkar, Ragan B. Robertson, and Julio M. Fernandez, Proc. Natl. Acad. Sci. U.S.A. **101**, 12882 (2004).
[13] Scott G. Flicker, Jennifer L. Tipa, and Stacy G. Bike, J. Colloid Interface Sci. **158**, 317 (1993).
[14] Jacob N. Israelachvili, *Intermolecular and Surface Forces with Applications to Colloidal and Biological Systems* (Acadmic Press, London, England, 1985).
[15] Richard A. L. Jones, *Soft Condensed Matter* (Oxford University Press, Oxford, England, 2002).
[16] Y. Zhu and S. Granick, Phys. Rev. Lett. **88**, 106102 (2002).
[17] Lakkapragada Suresh and John Y. Walz, J. Colloid Interface Sci. **196**, 177 (1997).
[18] Olga L. Vinogradova, Int. J. Min. Process. **56**, 31 (1999).